Aerospace Science and Technology 58 (2016) 156–165

Contents lists available at ScienceDirect

Aerospace Science and Technology

www.elsevier.com/locate/aescte

Study of droplets distribution on canopy of ringsail parachute in light rain

Jian Yue *, Puyun Gao, Wenke Cheng

College of Aerospace Science and Engineering, National University of Defense Technology, Changsha 410073, China

ARTICLE INFO

Article history:
Received 2 April 2016
Received in revised form 15 August 2016
Accepted 16 August 2016
Available online 20 August 2016

Keywords:
Ringsail parachute
DPM
Light rain
Droplets
Two-phase flow

ABSTRACT

As a basal part of the entire study of reliability performance of ringsail parachute and re-entry capsule descending in rain environment, droplets distribution characteristics on canopy surface are investigated firstly via two-phase flow approach in the paper. The model of ringsail parachute and capsule is built on the basis of the sizes of Chinese Shenzhou series spacecraft components. The simulation of droplet trajectories is implemented numerically using the Discrete Phase Model. The numerical simulations considering various rainfall rates and velocities of a ringsail parachute and capsule descending in light rain conditions are conducted. The results show that for one specific rainfall rate, there is a homologous critical value of descending speed of parachute and capsule, which is the dividing line between raindrops being trapped and not being trapped by the canopy; if the descending velocity is less than the critical value, no raindrops will be captured; in raindrops-trapped cases the raindrops are distributed on the bottom skirt zones of the canopy surface and not evenly distributed. The work in the paper will be helpful and significant for the further study of the effects of rain environment on the spacecraft recovery.

1. Introduction

Rainfall is a common natural phenomenon. However, when rainfall occurs, the manned space mission which includes rocket launch and spacecraft recovery will be delayed or canceled generally. Especially in the spacecraft recovery, the bad weather is more likely to bring unknown danger because the parachute, which is widely used to supply aerodynamic resistance to the spacecraft recovery, is quite sensitive to the weather conditions. Up to now almost all of the spacecraft recovery activities are carried out in good weather conditions. So it is of great significance to research the effects of rain condition on the performance of parachute for achieving the all-weather implementation of manned space mission. Chinese spacecraft landing area is located in a place where the rainfall is scarce most of the time. Light rainfall has a higher probability of occurrence compared with moderate and heavy rainfall. According to the local rainfall characteristics over the past years, light rain environment is considered in the paper. The research background of the paper can be introduced from the two aspects of ringsail parachute and rain.

Ringsail parachute has been widely applied in the aerospace area with its excellent performance. According to existent literatures, ringsail parachute has a better stability than some other types. It is because the gaps between the rings and sails are much more than others while the improved porosity can enhance stability of parachute. Also the ringsail parachute is more popular in the aerospace field due to its rather higher drag coefficient. It can provide enough resistance for the deceleration of re-entry capsule. So far a lot of research on the ringsail parachute has been carried out. Gao and Yu [1] researched the influence of reefing ratio on inflation performance of ringsail parachute and found that the reefing ratio was in linear relationship with the maximum opening load. Yang et al. [2] investigated the influence of permeability of fabric on aerodynamic performance of a ringsail parachute by establishing a new governing equation of flow considering the permeability of fabric. After comparing the numerical results with the traditional results they concluded that the new model was significant to improve the accuracy of flow field simulation. Stein and Tezduyar have achieved great success on the aspect of parachute fluid–structure interaction (FSI) in the past years [3–5]. The FSI modeling of a ringsail parachute for Orion space vehicle was studied in detail by Tezduyar et al. [6] and the results of a special case in which the influence of side winds was included were presented. In fact FSI has always been a focus of researching various types of parachute. Tutt and Taylor [7] used LS-DYNA to numerically simulate the inflation of parachute which was based on the Arbitrary Lagrangian Eulerian (ALE) Method. Kim et al. [8] modeled the evolution of parachute canopy and risers via using the

* Corresponding author.
E-mail address: kulouwang126@126.com (J. Yue).

http://dx.doi.org/10.1016/j.ast.2016.08.015
1270-9638/

front tracking method on a spring system. In addition there is also some FSI research of parachute and suspension line simulation via the immersed boundary (IB) method [9,10]. Most published literatures on the aspect of any types of parachute are generally aimed at studying the flow field, geometry, material characteristics or FSI problems. Until now, no directly relational literatures on the subject of descent of parachute in light rainfall environment are available.

Systematic research of rainfall has begun since more than half a century ago. In 1948 Marshall and Palmer [11] investigated the distribution of raindrops with size and gave its expression which was widely approved and adopted in the subsequent study of rain. Afterwards in 1976 an expression for the ground level and atmospheric raindrop size distribution was derived by Markowitz [12]. The later research concerning effects of rain is mainly concentrated in several fields, which include flight safety of aircraft, erosion of building surface and running safety of high speed train [13–15]. Particularly previous study on flight safety of aircraft is of great reference value to the subject in this paper. The research on flight safety of aircraft in rain environment began as early as in 1941 [13]. Then in 1983 Haincs and Luers [16] investigated the effects of heavy rain on aerodynamic penalties of landing aircrafts, and found the raindrop cratering and water film, which could produce drag increase of 5% to 10% for a 100 mm/h rain, were the causes of airfoil roughness. Afterwards Wan and Pan [17] carried out numerical simulation of aerodynamic efficiency of 2-D airfoil NACA64-210 under the influence of heavy rain via two-phase flow approach. In their study the raindrop trajectories were simulated by applying the discrete phase model (DPM) and the k–ε model was chosen as major turbulence model. The simulation results via two-phase flow approach were in good agreement with the experiment results obtained by Bezos and Campbell [18]. It is shown that in heavy rain environment the degradation of lift to drag ratio in average value was rather accurate compared with the experiment results. In recent years Ismail et al. [19] investigated the effects of heavy rain on the aerodynamic efficiency of 2D NACA 0012 airfoil and 3D NACA 0012 rectangular wing and the results showed significant increase in drag and decrease in lift in heavy rain condition. Also, in their study DPM was used to model the rain particles. These research papers indicate DPM of two-phase flow approach has been an approved and efficacious model to simulate the raindrop trajectories.

It is found from the foregoing statements that the influence of rain condition on performance of ringsail parachute has been rarely investigated up to now. The two-phase flow approach including DPM can be employed to deal with the involved problem. According to the principle of priority the raindrops distribution on canopy surface should be studied firstly before studying the effects of rain condition on the performance of parachute.

The ringsail parachute and capsule at high altitude has a higher descending velocity than the raindrops in the air according to the existing data. For example, when the average diameter of raindrops is 4 mm, which belongs to an uncommon heavy rainfall level, the descending velocity is about 9.550 m/s at the altitude of 2000 m. Meanwhile the descending velocity range of ringsail parachute and capsule is from 10 m/s to 30 m/s. One imaginary scene is that the ringsail parachute and capsule is chasing after the raindrops in the air. This means the research of descent of ringsail parachute and capsule in the rainfall is a little different from the study of aircraft flight. The relevant airdrop experiment is impracticable to conduct in the natural rain condition or in the indoor environment because of the difficulties of precise measurement of droplet parameters. So with progress in numerical modeling techniques, the numerical simulation, which is a comparatively reasonable way at present, is carried out in the paper. FSI is not considered because the shape of inflated canopy has been stable relatively when parachute and capsule entered the rainfall region at an altitude of no more than 5000 meters. In the simulation both the velocity conditions whether the raindrops can be trapped by the ringsail parachute canopy and the raindrops distribution on the canopy surface are studied.

The outline of the paper is as follows. Firstly the adopted mathematical and physical models are introduced. Then considering different rainfall rates and velocity conditions the two-phase flow approach is employed to simulate the descent of ringsail parachute and re-entry capsule in rain environment. Afterwards the results of distribution of raindrops are analyzed adequately. A summary of results analysis is provided in the last section.

2. Mathematical and physical model

2.1. Continuous phase model

In the two-phase flow approach the fluid is treated as a continuum. The descent of ringsail parachute is at a low speed of no more than 30 m/s in the paper. The incompressible Reynolds-averaged Navier–Stokes equations are solved for the continuous phase. The pressure-based segregated SIMPLE algorithm is employed to calculate the pressure-correlation equation. The second-order accurate scheme is implemented in the spatial discretization of pressure, momentum, energy and turbulence terms. The governing equations of flow field are written as

$$\frac{\partial \rho}{\partial t} + \frac{\partial \rho u_i}{\partial x_i} = 0 \tag{1}$$

$$\begin{aligned}\frac{\partial}{\partial t}(\rho u_i) + \frac{\partial}{\partial x_j}(\rho u_i u_j) &= -\frac{\partial p}{\partial x_i} + \frac{\partial}{\partial x_j}\left[\mu\left(\frac{\partial u_i}{\partial x_j} + \frac{\partial u_j}{\partial x_i} - \frac{2}{3}\delta_{ij}\frac{\partial u_l}{\partial x_l}\right)\right] \\ &\quad + \frac{\partial}{\partial x_j}\left(-\rho\overline{u_i' u_j'}\right)\end{aligned} \tag{2}$$

where ρ represents the density of fluid, u_i and u_j are the velocity components, p is pressure, $-\rho\overline{u_i' u_j'}$ represents the Reynolds stress term.

The Reynolds number of the flow field near the ringsail parachute is about $Re = 3.0 \times 10^7$ which indicates the turbulence model is needed. Owing to its reasonable accuracy for a wide range of turbulent flows, the k–ε model, which has been widely accepted in engineering applications, is adopted to model the turbulence. The k–ε model is commonly used to solve the turbulence in the past study of flow filed of parachute or raindrop trajectories [14,15,17,19,20]. It is a model on the basis of model transport equations for the turbulence kinetic energy k and its dissipation rate ε. The model transport equation for k is derived from the exact equation while the model transport equation for ε is obtained using some physical reasoning. The turbulence kinetic energy k and its dissipation rate ε can be obtained from the following transport equations [21]

$$\begin{aligned}\frac{\partial}{\partial t}(\rho k) + \frac{\partial}{\partial x_i}(\rho k u_i) &= \frac{\partial}{\partial x_j}\left[\left(\mu + \frac{\mu_t}{\sigma_k}\right)\frac{\partial k}{\partial x_j}\right] + G_k + G_b - \rho\varepsilon - Y_M + S_k\end{aligned} \tag{3}$$

$$\begin{aligned}\frac{\partial}{\partial t}(\rho \varepsilon) + \frac{\partial}{\partial x_i}(\rho \varepsilon u_i) &= \frac{\partial}{\partial x_j}\left[\left(\mu + \frac{\mu_t}{\sigma_\varepsilon}\right)\frac{\partial \varepsilon}{\partial x_j}\right] + C_{1\varepsilon}\frac{\varepsilon}{k}(G_k + C_{3\varepsilon}G_b) - C_{2\varepsilon}\rho\frac{\varepsilon^2}{k} + S_\varepsilon\end{aligned} \tag{4}$$

$$\mu_t = \rho C_\mu \frac{k^2}{\varepsilon} \tag{5}$$

Table 1
Values of some coefficients.

$C_{1\varepsilon}$	$C_{2\varepsilon}$	σ_k	σ_ε	C_μ
1.44	1.92	1.0	1.3	0.09

where G_k is the generation of turbulence kinetic energy, G_b is the generation of turbulence kinetic energy due to buoyancy, σ_k and σ_ε are the turbulent Prandtl numbers. Y_M represents the contribution of the fluctuating dilatation in compressible turbulence to the overall dissipation rate. μ_t represents turbulent viscosity. $C_{1\varepsilon}, C_{2\varepsilon}, C_{3\varepsilon}$ and C_μ are constants. S_k and S_ε are defined source terms. The values of some coefficients are listed in Table 1.

2.2. Discrete phase model

Following the Eulerian–Lagrangian approach the discrete phase model is established other than the continuous phase in two-phase flow model. The discrete phase will be solved by tracking a large number of particles in the calculated continuous phase [21]. In two-phase flow model the force of continuous phase can act on the discrete phase which has effects on the trajectories of particles. On the other hand the trajectories of particles have corresponding effects on the flow field. So the two-way coupling effects between continuous phase and discrete phase should be considered. The exchanges of mass, momentum and energy between the two phases are involved in the two-way coupled model. In the paper the discrete phase model considering two-way coupling effects is used to simulate the raindrop trajectories in the air. However, for simplification the collision, deformation and evaporation of raindrops are ignored. The trajectories of raindrops are calculated by integrating the force balance acting on the particles. It is written for the y direction in Cartesian coordinates in a Lagrangian reference frame as

$$\frac{\mathrm{d}u_r}{\mathrm{d}t} = F_D(u - u_r) + \frac{g_y(\rho_r - \rho_a)}{\rho_r} + F_y \tag{6}$$

where u_r is the raindrop velocity, u represents the velocity of air flow, g_y is the acceleration of gravity, ρ_r and ρ_a are the density of raindrop and air respectively, F_y is the additional force per unit mass, F_D is the drag force per unit mass, which can be given by

$$F_D = \frac{18\mu_a}{\rho_r D^2}\frac{C_D Re_r}{24} \tag{7}$$

$$C_D = \frac{k_1}{Re_r} + \frac{k_2}{Re_r^2} + k_3 \tag{8}$$

where μ_a represents the air molecular viscosity, D is the diameter of particle, C_D represents the drag force coefficient, k_1, k_2, k_3 are constants which are determined according to the range of Re_r [22]. Re_r represents the relative Reynolds number, which is defined as

$$Re_r = \frac{\rho_a D|u_r - u|}{\mu_a} \tag{9}$$

2.3. Physical model of raindrop

Rainfall is a complicated subject of research. The applicable physical model of raindrop for engineering has always been the target of researchers. In the pioneering research, based on experimental observations, Marshall and Palmer proposed a widely accepted formula of distribution of raindrops which is expressed as

$$N_D = N_0 \mathrm{e}^{-\Lambda D} \tag{10}$$

where D represents the raindrop diameter here, $N_D \bullet \delta D$ represents the number of raindrops of diameter between D and $D + \delta D$ in unit volume of space, $\Lambda = nR^m$, $N_0 = 8 \times 10^3\ \mathrm{m}^{-3}\,\mathrm{mm}^{-1}$, $n = 4.1$, $m = -0.21$ for light rain, R represents the rate of rainfall. With different R values the rain intensity is in four levels including light rain, moderate rain, heavy rain and storm rain. When $R \leq 2.5$ mm/h, the rain belongs to light rain level. Liquid Water Content (LWC), which represents the mass of the water per unit volume of air in g/m^3, is another measurement of intensity of rainfall. The value of LWC is calculated by

$$\mathrm{LWC} = \int_0^\infty \frac{\pi}{6}\rho_d D^3 N_0 \mathrm{e}^{-\Lambda D}\mathrm{d}D = \frac{N_0\rho_d\pi}{n^4 R^{4m}} \tag{11}$$

For light rain here [19],

$$\mathrm{LWC} = 0.08894R^{0.84} \tag{12}$$

In the study it is assumed all the raindrops are in spherical shape and uniform average sizes. From the following formula the mean equivalent volumetric diameter D_V can be obtained. It is regarded as the mean diameter of all raindrops.

$$D_V = \frac{\int_0^\infty D\frac{\pi}{6}D^3 N_0 \mathrm{e}^{-\Lambda D}\mathrm{d}D}{\int_0^\infty \frac{\pi}{6}D^3 N_0 \mathrm{e}^{-\Lambda D}\mathrm{d}D} = \frac{4}{nR^m} \tag{13}$$

Another important parameter of the physical model of raindrop is the terminal velocity. Due to the gravity and the drag force of air being in balance the raindrops will reach a rather steady speed in the terminal descent stage. The formula of final speed of a raindrop contains raindrop diameter and the density of local air. It has been developed by Markowitz as

$$V_D = 9.58\left[1 - \mathrm{e}^{-\left(\frac{D}{1.77}\right)^{1.147}}\right]\left(\frac{1.225}{\rho_a}\right)^{0.4} \tag{14}$$

3. Simulation

3.1. Geometry model and computational fluid domain

The ringsail parachute is modeled based on the profiles of Chinese Shenzhou series spacecraft components. The front view and top view are shown in Fig. 1. The ringsail parachute consists of 8 rings near the vent and 12 sails near the middle and skirt portions. These sails include 1152 pieces of fabric. There are gaps between neighboring rings or sails. The re-entry capsule is linked to the joints at the bottom edges of canopy using 96 suspension lines. Considering the thin size the suspension lines are ignored in the coming simulation of flow field for simplification. The detailed sizes and location relationships of ringsail parachute and capsule are shown in Fig. 2. The radius of vent is 0.77 m. The nominal radius of canopy is about 13 m. The height of inflated canopy is 12 m. The vertical distance between ringsail parachute and capsule is 50 m.

Only one quarter of the cylinder computational fluid domain is meshed because of the symmetry characteristics of the ringsail parachute and capsule. As is shown in Fig. 3, the boundary conditions for the computational fluid domain include velocity inlet boundary at the bottom of fluid domain, from which the airflow comes into the domain in a velocity; pressure outlet at the top, where the static pressure is specified; symmetry boundary at the side, where pattern of the flow has mirror symmetry; and no-penetration and no-slip wall boundary condition on the canopy and re-entry capsule surface, which bounds fluid and solid regions. The dimension of fluid domain is 235 m in height and 45 m along the radial direction, which is large enough for flow field to develop fully. Considering the structure complexity of ringsail parachute the tetrahedral elements, which belong to non-structured mesh, are used for the fluid volume cells. There are

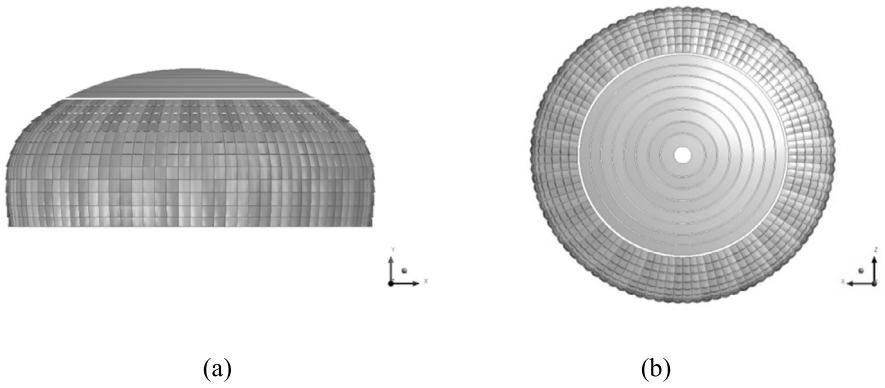

Fig. 1. View of ringsail parachute: (a) front view, (b) top view.

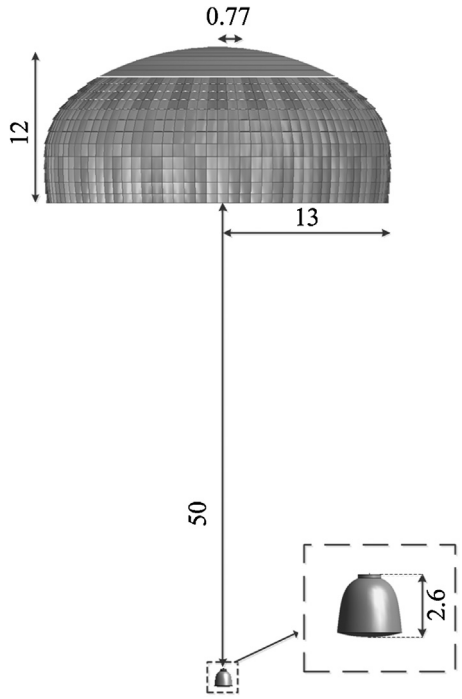

Fig. 2. Sizes of ringsail parachute and re-entry capsule (all dimensions are in meters).

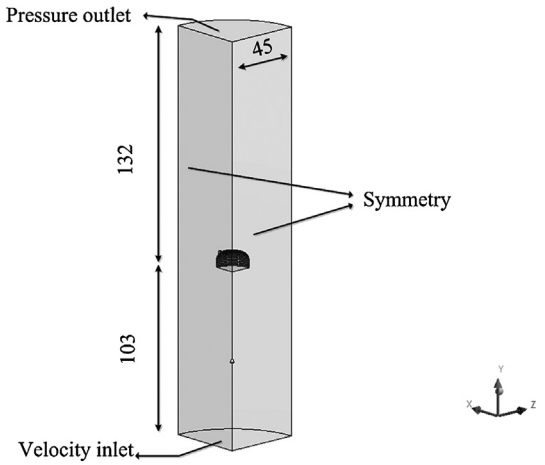

Fig. 3. Boundary conditions and sizes of computational fluid domain (all dimensions are in meters).

approximately 3,600,000 grid cells in total, which are shown in Fig. 4.

3.2. Computational parameters

The scene to be simulated is assumed that the ringsail parachute and re-entry capsule is descending vertically in the light rain environment at the altitude of 2000 m. The detailed parameters of local air referring to the US standard atmosphere [23] are adopted which are shown in Table 2. In the simulation the raindrops will come into the fluid domain through the velocity inlet face. The results of fore simulations indicate that merely the droplets injected from the projection zone of canopy on the bottom face are possible to reach onto the canopy surface. So the droplets injection points are only set on a bottom area which is a little larger than the projection zone of canopy on the velocity inlet face. This arrangement can economize on the computation resources. As is shown in Fig. 5, the area of injection zone is 16.2 m × 16.2 m. Multiplying the injection area by descending speed of ringsail parachute and LWC will be an important parameter of DPM, namely total mass flow rate (kg/s). The raindrops injection process is shown in Fig. 6. The raindrops are injected at a speed which is the velocity difference between the descending parachute and terminal raindrops.

The space between the injection points is determined according to the average distance between raindrops, which is represented by L_r. Table 3 shows the parameters of raindrops applied in the numerical calculation. For $R = 0.5$ mm/h, 1 mm/h and 2 mm/h there are totally 95×95, 91×91 and 82×82 injection points respectively set on the injection zone in light of L_r values.

If the injected raindrops arrive onto the capsule and canopy surface there are four possible regimes to describe the interaction between the raindrops and wall boundary which include stick, spread, rebound and splash. As is shown in Fig. 7, the interaction is an actually complex process which is based on the impact energy and wall temperature. For simplification it is assumed that when raindrops are trapped by the canopy surface the stick or spread regime is considered to occur. At this stage it is a reasonable assumption because the focus of the research is to study the distribution characteristics of droplets on the canopy.

What's more, the flow field of the parachute and the capsule will reach a relatively steady state ultimately after adopting transient algorithm for a calculation. It is because the inflating of canopy has already finished and the shape keeps stable when the ringsail parachute and capsule enters the raining district. So the flow field is considered steady.

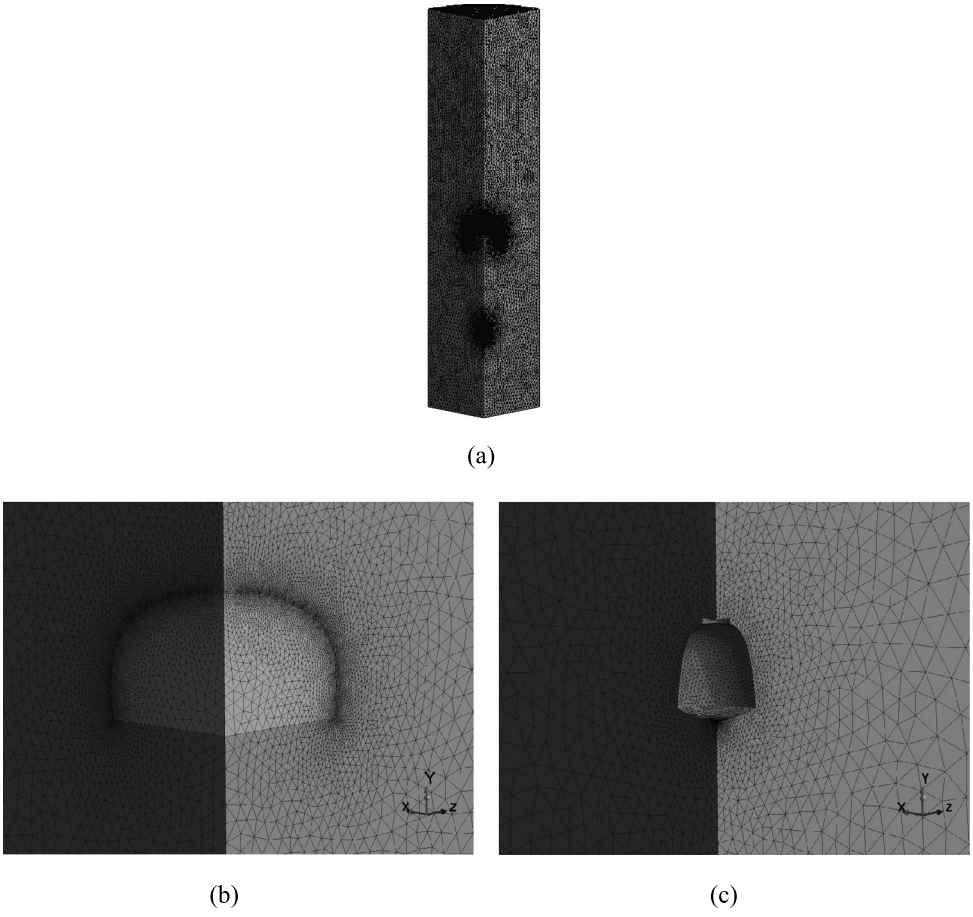

Fig. 4. Computational grid of (a) entire domain, (b) domain near the canopy, (c) domain near the re-entry capsule.

Table 2
Parameters of local air at the altitude of 2000 m.

ρ_a (kg/m^3)	μ (Pa s)	T (K)	P (Pa)
1.007	1.726×10^{-5}	275.15	7.95×10^4

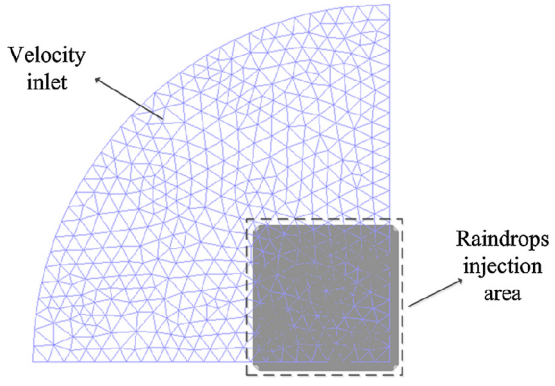

Fig. 5. Injection zone of raindrops.

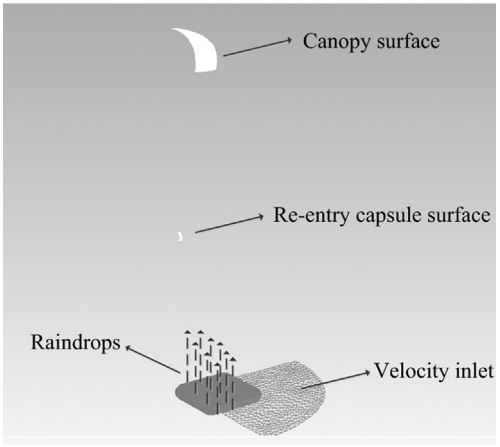

Fig. 6. Injection process of raindrops.

4. Results and discussion

4.1. Mesh independence study

Increment of grid numbers brings the enhancement of both computational accuracy and computational resources costing. In order to reduce the influence of grid numbers variation the mesh independence study is carried out. The cases that parachute and capsule is descending at rainfall rate 1 mm/h under four kinds of grid scales are calculated. As is shown in Table 4, no raindrops are trapped by canopy surface at the descending speed of 16 m/s, so the variation of grid numbers has no effect on these cases. The grid numbers variation has apparently caused the change of time-average raindrop numbers trapped by canopy surface at the descending speed of 22 m/s. The error difference of drag coefficient is less than 0.30% when the mesh number is greater than 3,600,000. The change of trapped raindrop numbers is also not obvious. The further refinement of grid density will be not significant. Ultimately the mesh scale of 3,604,201 is employed to continue calculating the remaining cases in light rain condition.

Table 3
Raindrops parameters at different rates of rainfall.

R (mm/h)	LWC (g/m^3)	D_V (mm)	L_r (cm)	V_D (m/s)
0.5	0.0497	0.8435	17.2	3.603
1	0.0889	0.9756	18.0	4.108
2	0.1590	1.1280	20.0	4.655

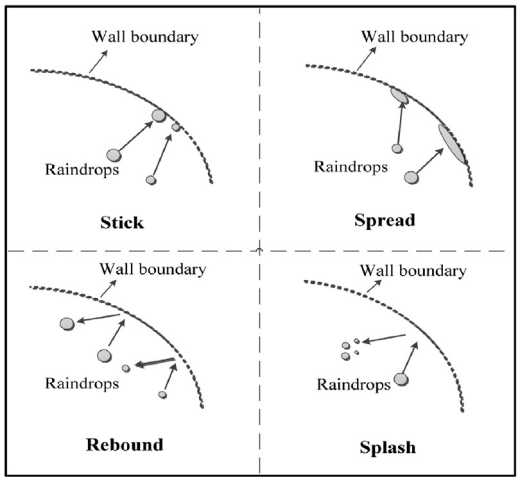

Fig. 7. Regimes of interaction at wall boundary.

Table 4
Results of four kinds of grid scales at rainfall rate 1 mm/h.

Mesh numbers	Velocity of flow inlet (m/s)	Raindrop numbers trapped by canopy surface	Drag coefficient	Error
3,014,320	16	0	0.733	–
3,604,201	16	0	0.720	−1.77%
4,147,406	16	0	0.722	+0.28%
4,444,339	16	0	0.721	−0.14%
3,014,320	22	1238	0.745	–
3,604,201	22	1260	0.734	−1.48%
4,147,406	22	1256	0.733	−0.14%
4,444,339	22	1272	0.731	−0.27%

4.2. Results presentation and analysis

Under various rainfall rates and descending velocities of ringsail parachute and capsule a lot of numerical simulation cases are calculated. Fig. 8 shows the common sample trajectories of raindrops. The color change represents the velocity variety of raindrops at different locations. Note that it is not a focus here. In Fig. 8(a) the raindrop moves from the bottom velocity inlet face to the upper outlet along the flow field of ringsail parachute and capsule. During this process the raindrop is not trapped by the canopy surface which is applicable to most raindrops. However, in Fig. 8(b) another raindrop is trapped by the canopy in the moving course. Fig. 8(c) shows the trajectories of all raindrops in a case while Fig. 8(d) shows the trajectories near the canopy from the view of

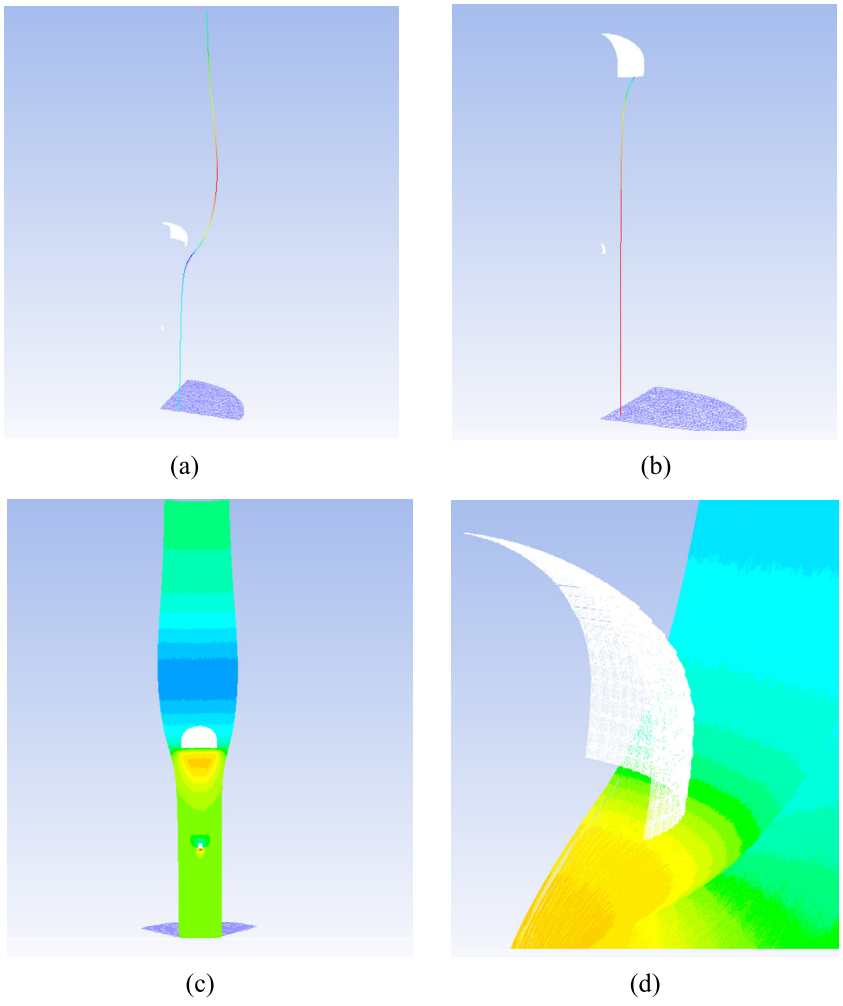

Fig. 8. Trajectories of (a) not trapped raindrops, (b) trapped raindrops, (c) all raindrops, (d) raindrops near the canopy.

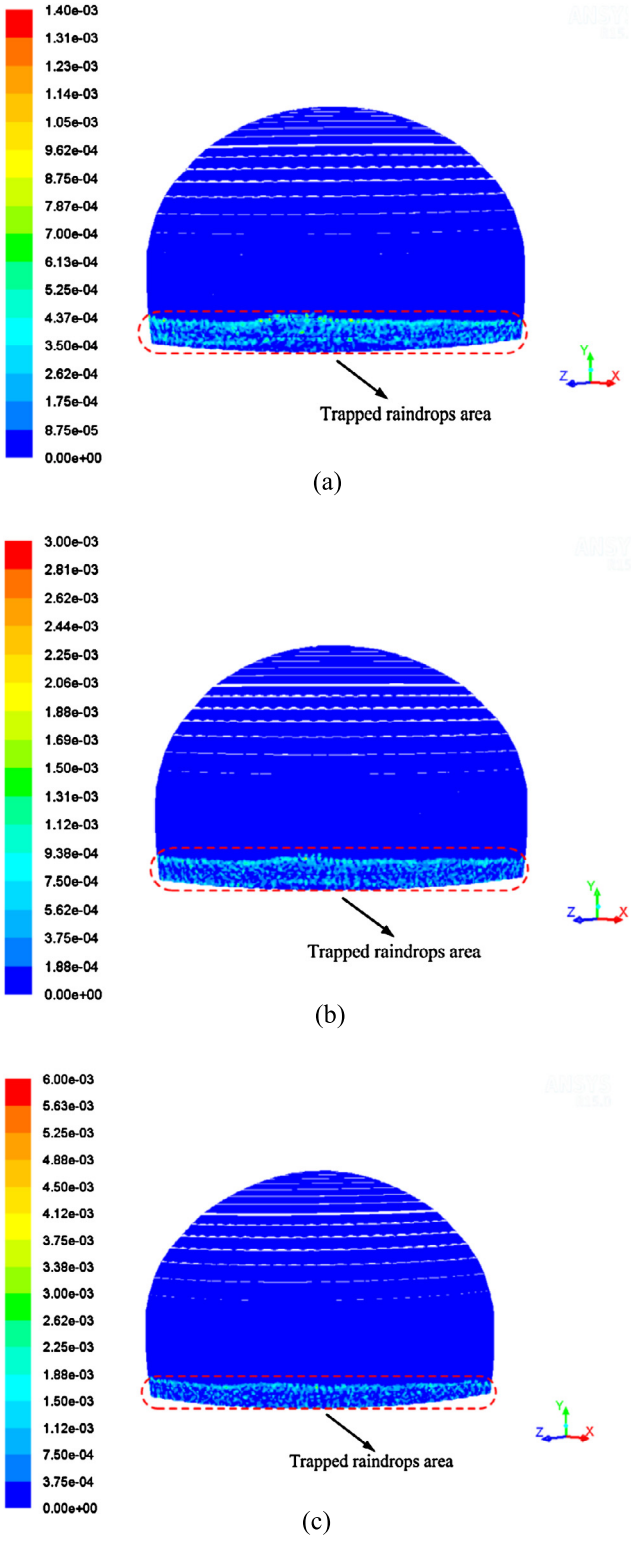

Fig. 9. Contours of trapped raindrops distribution on canopy at an inlet speed of 22 m/s when (a) $R = 0.5$ mm/h, (b) $R = 1$ mm/h, (c) $R = 2$ mm/h.

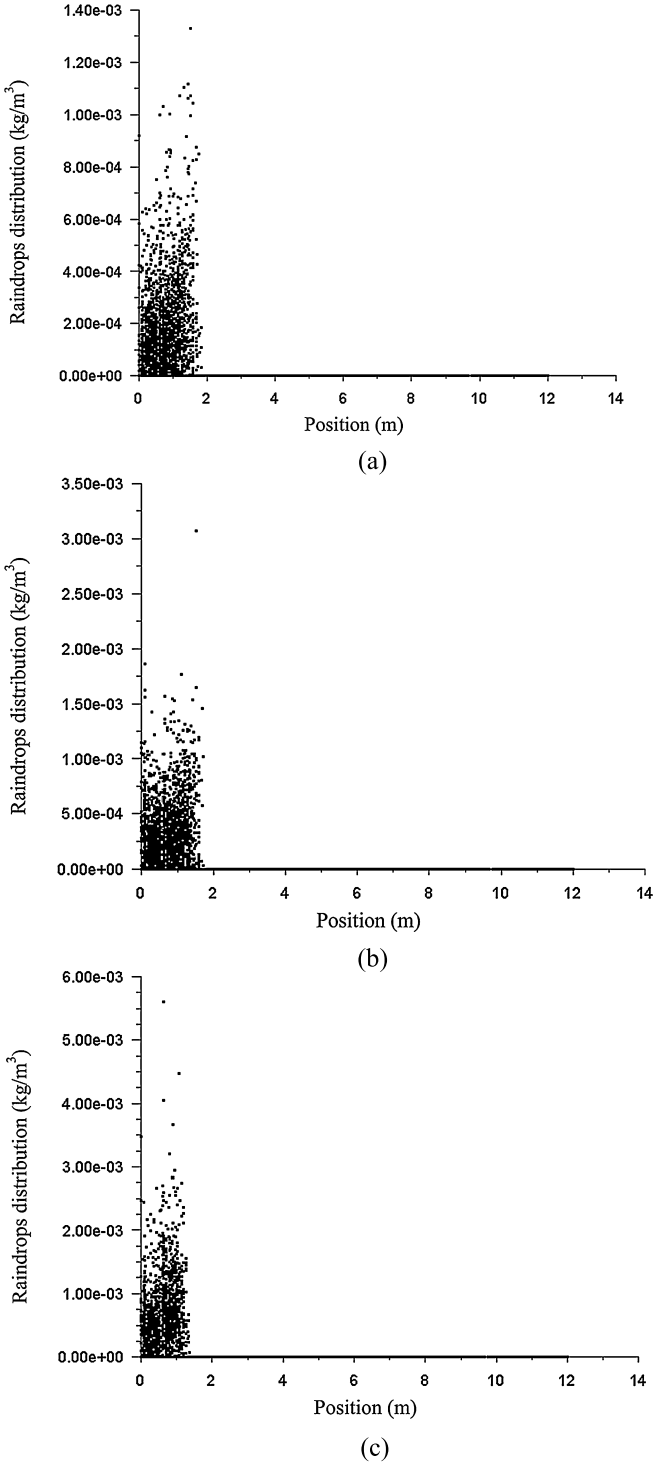

Fig. 10. Raindrops distribution along the Y+ direction at an inlet speed of 22 m/s when (a) $R = 0.5$ mm/h, (b) $R = 1$ mm/h, (c) $R = 2$ mm/h.

another angle. Of course a minority of raindrops can reach onto the capsule surface, but it is not the focus of research in the paper.

The simulation results indicate that when the descending speed of ringsail parachute is large enough there will be raindrops to be trapped by the canopy. Fig. 9 shows the contours of trapped raindrops distribution on the inner canopy surface when the descending velocity is 22 m/s at three rainfall rates. As is shown in the figures, the trapped raindrops are mainly concentrated on the bottom skirt part of canopy. Not the whole surface of canopy is distributed on by the trapped raindrops. For all raindrops-trapped cases there is a common law that the trapped raindrops are not evenly distributed on the canopy. Fig. 10 indicates that the trapped raindrops are distributed at a range of 2 m along the $Y+$ direction and the range decreases with the rainfall rate increasing. The numerical simulations are carried out without employing the turbulent dispersion model. It is because the fore calculation results

Table 5
Cases at $R = 0.5$ mm/h.

V (m/s)	N_p	m_f (kg/s)	N_t	m_t (kg/s)
10	9025	0.1304	0	0
14	9025	0.1826	0	0
16	9025	0.2087	0	0
17	9025	0.2217	13	3.111E−4
18	9025	0.2348	279	7.267E−3
20	9025	0.2609	1047	3.027E−2
22	9025	0.2870	1395	4.438E−2

Table 6
Cases at $R = 1$ mm/h.

V (m/s)	N_p	m_f (kg/s)	N_t	m_t (kg/s)
10	8281	0.2333	0	0
14	8281	0.3266	0	0
16	8281	0.3733	0	0
17	8281	0.3966	0	0
18	8281	0.4200	23	1.167E−3
20	8281	0.4666	751	4.233E−2
22	8281	0.5133	1260	7.812E−2

Table 7
Cases at $R = 2$ mm/h.

V (m/s)	N_p	m_f (kg/s)	N_t	m_t (kg/s)
10	6724	0.4173	0	0
14	6724	0.5842	0	0
16	6724	0.6676	0	0
17	6724	0.7094	0	0
18	6724	0.7511	0	0
20	6724	0.8346	370	4.588E−2
22	6724	0.9180	869	1.187E−1

show the range of wet zone considering the turbulent dispersion is only a little bigger than that without considering the turbulent dispersion, which has no effect on the conclusions in the paper.

The detailed statistic results of various cases are listed in Table 5, Table 6 and Table 7 for rainfall rate 0.5 mm/h, 1 mm/h and 2 mm/h respectively, where V is the velocity of airflow inlet which represents the descending speed of ringsail parachute and re-entry capsule, N_p is the numbers of distributed injection points, m_f is the total mass flow rate, N_t is the mean raindrop numbers trapped by canopy surface, m_t is the mean raindrop mass trapped by canopy surface. It can be concluded from the tables that in the cases where the descending speed is less than 16 m/s, no raindrops are trapped by the canopy, which means the influence of raindrops on the parachute can be neglected under this condition. There is a dividing line of descending speed of parachute and capsule for different rainfall rates. Only when the descending speed is greater than the critical value can part of raindrops be captured by the canopy surface. And the critical value of descending speed is different at various rainfall rates. As the rainfall rates increase the critical values also become larger. In raindrops-trapped cases the mass of trapped raindrops increases with the growth of rainfall intensity for an identical descending speed. For example, when the velocity of airflow inlet is 22 m/s, the mass of trapped raindrops is 4.438E−2 kg/s, 7.812E−2 kg/s and 1.187E−1 kg/s at rainfall rate 0.5 mm/h, 1 mm/h and 2 mm/h respectively.

A high pressure zone exists under the canopy surface in the flow field. The high pressure decreases the vertical velocity of raindrops and gives a horizontal velocity. Then most of the raindrops deflect because of the horizontal effects on the raindrops, which could be found in Fig. 8. So only a small portion of the canopy surface traps raindrops. The velocity difference in the vertical direction between the canopy and raindrops plays an important role in the development of traces of raindrops. For an identical rainfall rate the relative speed becomes larger with the increase of descending speed of ringsail parachute. The alteration adds the difficulties of transforming the momentum of raindrops in horizontal direction. So in cases where the inlet velocity of airflow is larger the raindrops are more possible to be trapped. The terminal velocity of raindrops grows with the increase of rainfall rate. This means that larger descending speed is needed to ensure there will be raindrops to be captured at higher rainfall rates. Then the increase of critical values of descending speed of ringsail parachute, which determines whether or not the raindrops are trapped by canopy surface, can be explained. According to Eq. (14) the terminal speed of raindrops increases with the growth of raindrops diameters. For an identical descending speed of ringsail parachute the relative velocity between the canopy and raindrops becomes smaller with the growth of rainfall rates. Then in higher rainfall rate cases the trajectories of raindrops are easier to deflect which brings about the reduction of raindrops distribution areas on the canopy.

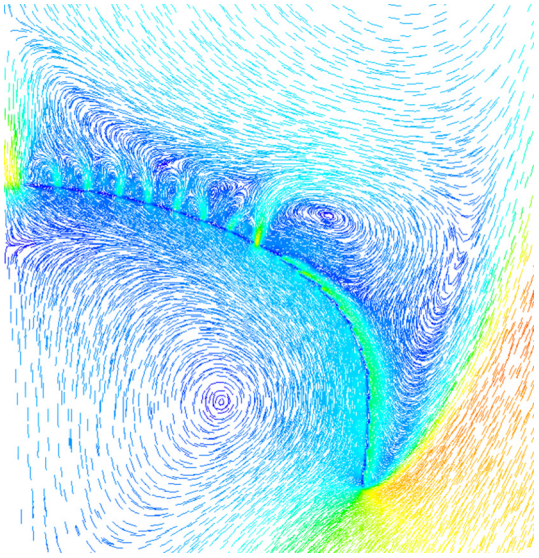

Fig. 11. Streamlines of flow field near the canopy.

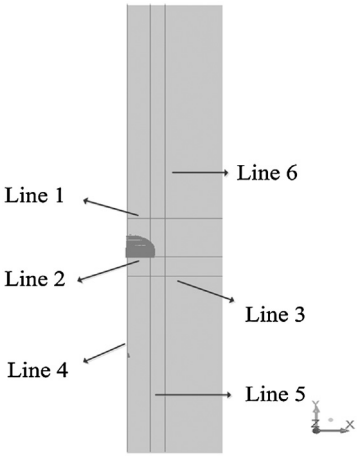

Fig. 12. Positions of chosen three horizontal and three vertical lines.

However, the basic factors to affect the trajectories of raindrops are the pressure and velocity distribution of flow field. Fig. 11 shows the contours of streamlines near the canopy in a slice plane. The color change in Fig. 11 represents the velocity variety of airflow which is not a focus here. There is a large vortex enclosed by the windward face of canopy. The formation of this vortex is due to the blocking effect of canopy. A minority of air flows through

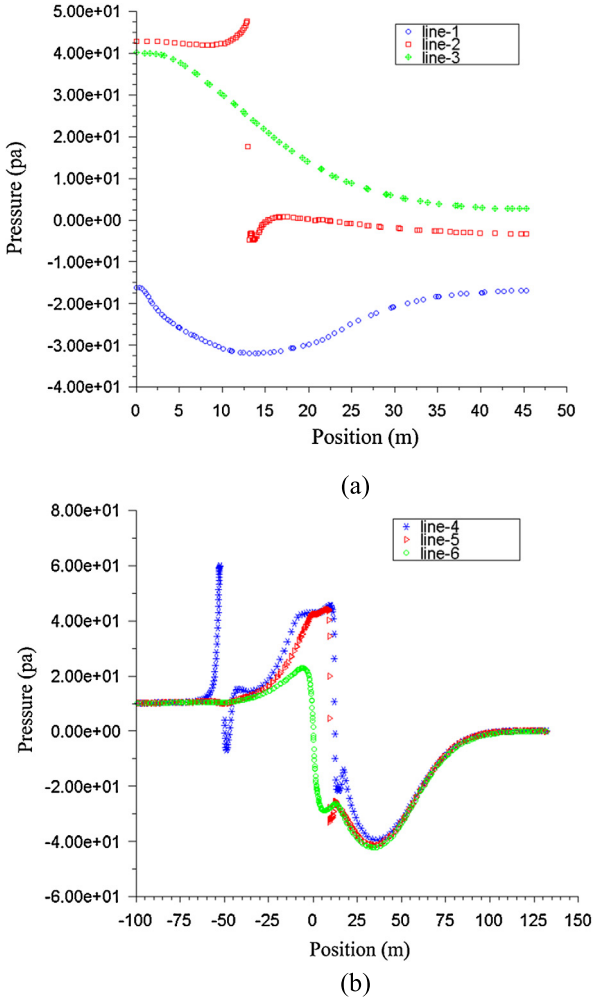

Fig. 13. Static pressure variation (a) along the horizontal lines, (b) along the vertical lines.

the gaps between the rings and sails and leads to the formation of some jets. The airflow grows into several small vortices on the leeward surface of canopy under the shear effects of near jets. As is shown in Fig. 12, three horizontal and three vertical lines across a slice plane of the whole flow field are chosen to reveal the variety of pressure field. It is found from Fig. 13 that the pressure under the canopy is higher than other zones due to the resistance effect of canopy. When airflow approaches the canopy the pressure is in a rising tendency. Then a low pressure zone emerges because at a distance above the canopy leeward side there is another large vortex due to the separation effect of canopy edge. In the zone farther from the canopy surface the pressure starts to increase. As is shown in Fig. 14, the speed of airflow is decelerated in the high pressure zone. The velocity of raindrop particles will be also decelerated and a horizontal effect will be applied to the particles when raindrops go through the high pressure region. In conclusion the raindrops distribution characteristics on the canopy surface are a result of a variety of effects in the flow field.

The numerical method to simulate the rain environment employed in this paper is the same as some other published literatures on the study of aircraft performance in heavy rain. In their paper the two-phase flow approach has been proved to be an effective method by comparing the numerical and experimental results, which indicates indirectly that the simulation results in our paper have a certain reference value. However, there are still some limitations of study in the paper, such as complicated physical processes of raindrops are neglected, water absorption saturation of canopy materials is not considered, no related experimental data is available and so on. In addition, further study is needed to continue the research in this area, for example, study of the accumulation of the rain impacts, the shape change after the canopy materials being wet. And the research methods are not limited to CFD.

5. Conclusions

A ringsail parachute and re-entry capsule model descending in a light rain environment is numerically simulated via the two-phase flow approach. The droplets distribution characteristics on the canopy surface are researched which belongs to a preliminary stage of the whole research of the reliability performance of

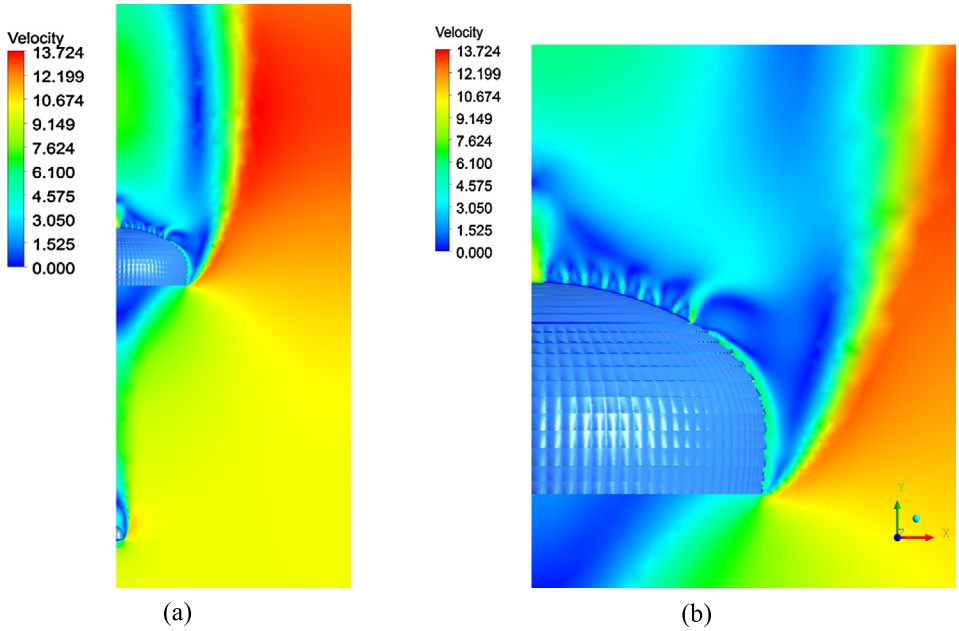

Fig. 14. Velocity field (a) on the entire slice, (b) near the canopy.

ringsail parachute and capsule descending in rain condition. The simulation results of various cases are presented and analyzed. It is found that for one given rainfall rate, there is a homologous critical value of descending velocity of parachute and capsule, which has a decisive influence on the raindrops being trapped or not being trapped by the canopy; if the descending velocity is less than the critical value, no raindrops will be trapped; in raindrops-trapped cases the raindrops are only unevenly distributed on the bottom skirt zones of the canopy surface. However, the experimental results are still needed to directly validate the simulation results in the future when the experiment conditions are fulfilled.

Conflict of interest statement

The author(s) declared no conflicts of interest.

References

[1] S.Y. Gao, L. Yu, Influence of reefing ratio on inflation performance of ringsail parachute, Chin. Space Sci. Technol. 1 (2014) 63–70, http://dx.doi.org/10.3780/j.issn.1000-758X.2014.01.009 (in Chinese).

[2] X. Yang, L. Yu, Y.W. Li, Y.J. Li, Numerical simulation of the effect of the permeability on the ringsail parachute in terminal descent stage, Acta Aerodyn. Sin. 33 (5) (2015) 714–719, http://dx.doi.org/10.7638/kqdlxxb-2014.0081 (in Chinese).

[3] K. Stein, R. Benney, T.E. Tezduyar, J. Potvin, Fluid–structure interactions of a cross parachute: numerical simulation, Comput. Methods Appl. Mech. Eng. 191 (6–7) (2001) 673–687, http://dx.doi.org/10.1016/S0045-7825(01)00312-7.

[4] T.E. Tezduyar, Y. Osawa, Fluid–structure interactions of a parachute crossing the far wake of an aircraft, Comput. Methods Appl. Mech. Eng. 191 (6–7) (2001) 717–726, http://dx.doi.org/10.1016/S0045-7825(01)00311-5.

[5] T.E. Tezduyar, S. Sathe, R. Keedy, K. Stein, Space–time finite element techniques for computation of fluid–structure interactions, Comput. Methods Appl. Mech. Eng. 195 (17–18) (2006) 2002–2027, http://dx.doi.org/10.1016/j.cma.2004.09.014.

[6] T.E. Tezduyar, S. Sathe, M. Schwaab, J. Pausewang, J. Christopher, J. Crabtree, Fluid–structure interaction modeling of ringsail parachutes, Comput. Mech. 43 (2008) 133–142, http://dx.doi.org/10.1007/s00466-008-0260-8.

[7] B.A. Tutt, A.P. Taylor, The use of LS-DYNA to simulate the inflation of a parachute canopy, in: 18th AIAA Aerodynamic Decelerator Systems Technology Conference and Seminar, 2005.

[8] J.D. Kim, Y. Li, X.X. Li, Simulation of parachute FSI using the front tracking method, J. Fluids Struct. 37 (2013) 100–119, http://dx.doi.org/10.1016/j.jfluidstructs.2012.08.011.

[9] Y. Kim, C.S. Peskin, 3-D Parachute simulation by the immersed boundary method, Comput. Fluids 38 (2009) 1080–1090, http://dx.doi.org/10.1016/j.compfluid.2008.11.002.

[10] X.P. Xue, H. Koyama, Y. Nakamura, C.Y. Wen, Effects of suspension line on flow field around a supersonic parachute, Aerosp. Sci. Technol. 43 (2015) 63–70, http://dx.doi.org/10.1016/j.ast.2015.02.014.

[11] J.S. Marshall, W.M. Palmer, The distribution of raindrops with size, J. Meteorol. 5 (4) (1948) 165–166.

[12] A.H. Markowitz, Raindrop size distribution expressions, J. Appl. Meteorol. 15 (9) (1976) 1029–1031.

[13] R.V. Rhode, Some effects of rain fall on flight of airplanes and on instrument indications, NACA TN-903, 1941.

[14] W. Tang, C.I. Davidson, Erosion of limestone building surfaces caused by wind-driven rain, 2: numerical modeling, Atmos. Environ. 38 (2004) 5601–5609, http://dx.doi.org/10.1016/j.atmosenv.2004.06.014.

[15] T.V. Hooff, B. Blocken, M.V. Harten, 3D CFD simulations of wind flow and wind-driven rain shelter in sports stadia: influence of stadium geometry, Build. Environ. 46 (2011) 22–37, http://dx.doi.org/10.1016/j.buildenv.2010.06.013.

[16] P.A. Haines, J.K. Luers, Aerodynamic penalties of heavy rain on landing airplanes, J. Aircr. 20 (2) (1983) 111–119, http://dx.doi.org/10.2514/3.44839.

[17] T. Wan, S.P. Pan, Aerodynamic efficiency study under the influence of heavy rain via two-phase flow approach, in: Proceedings of 27th International Congress of the Aeronautical Sciences, 2010.

[18] G.M. Bezos, B.A. Campbell, Development of a large-scale, outdoor, ground-based test capability for evaluating the effect of rain on airfoil lift, NASA TM-4420, 1993.

[19] M. Ismail, Y.H. Cao, A. Bakar, Z.L. Wu, Aerodynamic efficiency study of 2D airfoils and 3D rectangular wing in heavy rain via two-phase flow approach, Proc. ImechE, Part G, J. Aerosp. Eng. 228 (7) (2014) 1141–1155, http://dx.doi.org/10.1177/0954410013486406.

[20] D. Mazyar, D. Abdolrahman, H. Amir, A numerical and experimental study of the aerodynamics and stability of a horizontal parachute, ISRN Aerosp. Eng. 2013 (2013) 1–8, http://dx.doi.org/10.1155/2013/320563.

[21] Fluent Inc., Fluent Theory Guide, 2005.

[22] S.A. Morsi, A.J. Alexander, An investigation of particle trajectories in two phase flow systems, J. Fluid Mech. 55 (1972) 193–208.

[23] NOAA US, Force USA, US Standard Atmosphere, US Government Printing Office, Washington, DC, 1976.